

Article

Next-Generation Cellulosic Filaments from Hemp Pulp via Dry-Jet Wet Spinning Using HighPerCell[®] Technology

Antje Ota ^{1,*}, Marc Philip Vocht ¹, Ronald Beyer ¹, Anne Reboux ², Charles Reboux ² and Frank Hermanutz ¹

¹ German Institutes of Textile and Fiber Research Denkendorf (DITF), 73770 Denkendorf, Germany; marcphilip.vocht@ditf.de (M.P.V.); ronald.beyer@ditf.de (R.B.); frank.hermanutz@ditf.de (F.H.)

² RBX Créations, 17520 Neuillac, France; anne.reboux@iroony.net (A.R.); manager@gorfoo.net (C.R.)

* Correspondence: antje.ota@ditf.de

Abstract: Fiber demand of cellulosic fibers is rapidly increasing; however, these fibers are mainly based on the use of wood pulp (WP), which often have long transport times and, consequently, a high CO₂ footprint. So, alternative pulps based on non-wood, annual fast-growing plants are an option to cover the demand for raw materials and resources. Herein, we report on the use of a novel developed hemp pulp (HP) for man-made cellulosic fiber filament spinning. Commercial WP was used as a reference material. While HP could be used and directly spun as received without any further pre-treatment, an additional step to adjust the degree of polymerization (DP) was needed to use the wood pulp. Continuous filaments were spun using a novel dry-jet wet spinning (HighPerCell[®] process) technique, which is based on the use of 1-ethyl-3-methylimidazolium octanoate ([C₂C₁im][Oc]) as a solvent. Via this approach, several thousand meters (12,000 m–15,000 m) of continuous multifilament filaments were spun. The HP pulps showed excellent spinning performance. The novel approach allows the preparation of cellulosic fibers for either technical—with high tensile strength—or textile—possessing a low fibrillation tendency—applications. Textile hemp-based filaments were used for first weaving trials, resulting in a flawless fabric.

Keywords: hemp; cellulose; ionic liquid; dry-jet wet spinning; man-made cellulose fibers



Citation: Ota, A.; Vocht, M.P.; Beyer, R.; Reboux, A.; Reboux, C.; Hermanutz, F. Next-Generation Cellulosic Filaments from Hemp Pulp via Dry-Jet Wet Spinning Using HighPerCell[®] Technology. *Fibers* **2023**, *11*, 90. <https://doi.org/10.3390/fib11110090>

Academic Editors: Catalin R. Picu and Lucian Lucia

Received: 13 September 2023

Revised: 9 October 2023

Accepted: 12 October 2023

Published: 26 October 2023



Copyright: © 2023 by the authors. Licensee MDPI, Basel, Switzerland. This article is an open access article distributed under the terms and conditions of the Creative Commons Attribution (CC BY) license (<https://creativecommons.org/licenses/by/4.0/>).

1. Introduction

Plant-based materials have been a part of human life for thousands of years, and hemp in particular is widely used around the world. Strong and resilient, hemp was used mainly for textiles, medicines, and paper until the early 20th century when it was slowly replaced by petrochemical fibers and other materials, such as wood and cotton [1,2]. This is illustrated by the fact that the total area under cultivation in France fell from around 180,000 hectares in 1850 to less than 1000 hectares in 1960. Hemp textiles almost completely disappeared, and only a few countries, such as Romania and China, maintained small-scale industrial production. In recent decades, issues such as global warming, environmental abuse, and climate drift inspired some farmers and companies to start growing hemp again for new applications, such as construction, technical paper, food, and cosmetics. In 2022, France remained the main producer of hemp in Europe, with 22,000 ha under cultivation (40% of total EU production), of which 1800 ha was used for seed production [3].

Cotton currently has the largest market share of natural cellulose-based textile fibers. Forecasts assume that global annual textile fiber production is expected to increase from 113 million tons in 2021 to 133.5 million tons by 2030, while cotton production will remain static at between 26 and 28 million tons annually [4]. The resulting “cellulose gap” must be closed by increasing the use of wood-based pulp and through the identification of additional cellulosic sources, such as annual plants, waste streams, and recycled cotton-rich fabrics [5,6]. The production of dissolving pulp from wood requires a great deal of time for the trees to grow. Instead of using only the bast fiber process to turn the stalks of

annual plants into textiles, the cellulose can also be extracted and used to spin man-made cellulosic fibers (MMCFs). MMCFs production was revived in several reviews, and the different processes were compared [6–9]. Overall, the Viscos process, where cellulose is derived using toxic chemicals like CS₂, is the major MMCF-spinning technology. Lyocell is based on a direct solvent for cellulose and is a minor spinning process, as well as the most environmentally friendly [9]. Current trends include the development of filaments using new solvents like ionic liquids. However, the filament spinning—endless fiber—of MMCFs is still a challenge for the mentioned processes so further research has to be undertaken.

Pulps from annual crops such as hemp, flax and wheat or rice straw offer a more rapid increase in pulp volume due to the higher growth rate of the plants [10–12]. In addition, all of these fast-growing crops are considered to have a high potential for carbon sequestration [13,14]. However, agriculture is a major emitter of greenhouse gases, with 9.3 billion tons of eq. CO₂ emitted in 2018. In addition to deforestation and livestock-related emissions, mechanized agriculture using large quantities of chemical fertilizer is a major source of pollution and greenhouse gas emissions (mainly nitrous oxide) [15]. In this context, using straw for pulping must be considered carefully. According Da Silva et al., the biogenic emissions of methane are reduced via the removal of rice straw from the field. In contrast, a higher amount of fertilizers is needed to preserve the yield of harvested rice, causing increased nitrous oxide and carbon dioxide emissions [16]. Hemp, on the other hand, which is grown in rotation cycles, is a crop that requires little to no fertilizer and no pesticides or herbicides while producing up to 7.3 tons (source: Interchanvre) of biomass per hectare per year. This makes hemp a good alternative to wood, reducing the global footprint of the pulp industry while supporting sustainable agriculture. However, new processing steps are required for pulp purification, and its quality needs to be adapted by developing new approaches for pulp production.

Paulitz et al. [10] described the extraction of cellulose from hemp using aqueous caustic soda. For about one hour, the plant fibers were treated with caustic soda at 160 °C, followed by the addition of a combination of caustic soda and surface-active additives as a cooking liquor. Alternatively, the pulp was treated for 120 min at 55 °C with sodium hypochlorite and hydrogen peroxide, respectively. We used procedures to add the sequestrant for the elutriation of metal ions, which was necessary due to the followed Lyocell spinning process. The Lyocell process is based on the dissolution of cellulose in *N*-methylmorpholine-*N*-oxide (NMMO), which is unstable in the presence of metal ions, especially iron [17]. The resulting staple fibers showed good mechanical properties and were used for yarn spinning. The yarns obtained were comparable to convincing viscose yarns in terms of their mechanical properties and evenness. Thümmeler et al. later used hemp shives, a side product of hemp cultivation, for pulp preparation using a sulfur-free alkaline process at over 170 °C, followed by washing and bleaching steps [18]. The prepared fibers and filaments showed acceptable mechanical properties, comparable to industrial wood-based Lyocell fibers. Instead of using hemp plants directly for pulp production, a research group at Aalto University ground hemp fabrics for fiber spinning [19]. Before grinding, the fabrics were laundered to mimic a post-customer fabric and adjust the DP of the cellulose treated with H₂SO₄. As direct solvent 1,5-diazabicyclo[4.3.0]non-5-enium acetate ([DBNH][OAc]), an ionic liquid (IL) was used. The resulting MMCFs and the original hemp fibers differed not only in terms of their mechanical properties but also their structural properties. Like NMMO, ILs are direct solvents for cellulose, and the spinning process is comparable [20]. This makes the spinning of cellulosic fibers less laborious than the viscose process, which requires an additional chemical modification of the cellulose. Although NMMO is already used on a technical scale in the Lyocell process, ILs are said to be safer than NMMO, provided that the physico-chemical properties are carefully selected. Apart from [DBNH][OAc], there are other ILs, like imidazolium-based ILs, suitable for fiber spinning. We previously used 1-ethyl-2-methyl imidazolium octanoate [EMIM][Oct] as a solvent [21]. Compared to the other processes, the spinning of filament yarns is possible. This research focuses on investigating the use of two types of pulp, namely a wood pulp and a novel hemp pulp from RBX, for

textile filament spinning. RBX Créations has developed and patented a process, registered under the trademark Ironoxy[®], which allows mature hemp stalks to be processed into pulp, regardless of the harvesting system or retting method. Indeed, after seed harvesting, the hemp straw is a mixture of a woody core called hurd (50%), bast fiber (30%), and dust and fines (20%) [3]. The bast fibers can be primary fibers and tow with different finenesses and lengths. At the beginning of the pulping process, the feedstock, composed of different amounts of these elements (at least 30% hurd), is refined and washed at a temperature between 70 and 200 °C. The main objective is to obtain the purest pulp possible for the dissolving pulp market while reducing the need for chemical delignification.

2. Materials and Methods

2.1. Materials

Hemp pulp (HP) produced by RBX Créations was used for filament spinning. For this work, the farming group Chanvre Mellois, located in Aquitaine, France, provided the hemp stalks. Dissolving wood pulp (WP) was used as the commercial reference material. Technical-grade 1-ethyl-3-methylimidazolium octanoate ([C₂C₁im][Oc]) was supplied by IoLitec-Ionic Liquids Technologies GmbH (Heilbronn, Germany).

2.2. Pulp Preparation (RBX)

The thermo-mechanical pulping of the shredded and dried hemp was carried out in a cylindrical stainless-steel reactor using a temperature program between 30 and 220 °C. The pulping process was a new method developed on hemp (patent FR2000801).

2.3. R-18 Value

The cellulose content was determined using alkali resistance measurements. The residue unable to dissolve in 18 wt. % sodium hydroxide solution was measured according to DIN 54355 [22,23].

2.4. Ash Content

The ash content was determined gravimetrically after heating the samples to 575 °C and maintaining the temperature for 6 h according to DIN 54370 [24].

2.5. Elemental Analysis

Elemental analysis (EA) was carried out with a Perkin Elmer Analyzer 240. The measurements were performed at the Institute of Inorganic Chemistry of the University of Stuttgart, Germany. The determination of the metal ion content was conducted according to DIN EN ISO 11885 [25] using the ICP-OES instrument ICAP 7400 provided by Thermo Fisher Scientific (Waltham, MA, USA) [26].

2.6. Gel Permeation Chromatography

Gel permeation chromatography (GPC) was performed using an Agilent Infinity 1260 GPC, operated at 80 °C, combined with an Agilent (RI and viscosity) multidetector, operated at 40 °C. A PLgel mixed-B pre-column and PLgel mixed-B separation column (linear separation range: 500–10,000,000 g·mol⁻¹) were used. DMAc/LiCl (9 g·L⁻¹) was used as a solvent (flow rate 0.75 mL·min⁻¹). A conventional calibration versus Pullulan standards (PSS Mainz, Mn = 342–1,330,000 g·mol⁻¹) was applied. For sample preparation, 80 mg of the milled pulp was swollen once in water (12 h) and 3 times in DMAc (2 h). Each step was treated for 15 min in an ultrasonic bath. Then, the swollen pulp was dissolved in 5 mL DMAc/LiCl 90 g·L⁻¹ within 12 h at room temperature. Next, 1 mL of the solution was diluted with 1 mL DMAc and filtered through a poly(tetrafluoroethylene) membrane filter (0.45 µm). Similar procedures for GPC measurements are described in the literature [22,27]. The mass average molar mass (M_w), number average molar mass (M_n), and dispersity (\mathcal{D}) were calculated for all cellulose pulps. The dispersity is a measure for the width of a

molar mass distribution, and it is calculated from the ratio of the weight average to the number average.

$$D = \frac{M_w}{M_n} \quad (1)$$

2.7. Degree of Polymerization

The degree of polymerization (DP) of the cellulose was measured according to DIN 54270 [28]. The viscosimeter was equipped with a Schott Geräte GmbH Type Ia Ubbelohde. Samples were dissolved in an alkaline solution of the Fe (III) tartaric acid-sodium-complex. A detailed description is provided elsewhere [21].

2.8. Dope Preparation

The spinning dope concentration for all trials was 12 wt. % of cellulose in ionic liquids. The pulps were dissolved in [C₂C₁im][Oc] using a thin-film evaporator (VTA GmbH and Co. KG, Niederwinkling, Germany) at 120 °C and 60 mbar. The degassed dope was stored in a pressure filtration cauldron (Karl-Kurt Juchheim Laborgeräte GmbH, Bernkastel-Kues, Germany).

2.9. Rheological Measurements

To determine the rheological properties of the spinning dope, dynamic oscillatory experiments were performed (shear rate: 0.1 and 100 s⁻¹, deformation of 10%, temperature 20–110 °C) using a MCR 301 rheometer (Anton Paar, Graz, Austria). A Peltier temperature-control system and parallel-plate geometry (diameter 25 mm) with a gap of 1 mm was used. Storage, loss modulus, and complex viscosity were determined using the frequency-temperature superposition principle. Based on the Carreau Gahleitner model, zero shear viscosity was calculated [29].

2.10. Dry-Jet Wet Spinning

Multi-filament spinning was performed with a laboratory-scale device at 65 °C and 75 °C, respectively. The dope was passed through a filter with a mesh size of 0.043 mm. The extruder was heated and propelled the spinning dope to the 64-hole (capillary diameter = 150 µm) spinneret into a coagulation bath (water at 18 °C). Filaments were running through two washing baths and two washing godets and dried on a heated godet (90 °C) before being wound onto a bobbin. In total, 99.9% of the ionic liquid was recovered via the distillation of the water at 60 °C and 200 mbar.

2.11. Scanning Electron Micrograph

Scanning electron micrograph images of the imaging of the fiber surface and cross sections were recorded on a field emission scanning electron microscope (Zeiss Auriga). All samples were sputtered with Pt/Pd before the analysis.

2.12. Fiber Testing

Mechanical single-fiber analyses, such as tensile strength (cN/tex), elongation at break (%), Young's modulus (cN/tex), and fineness (dtex), were measured according to DIN EN ISO 5079 (20 individual measurements) using a Favimat+ from Textechno [30]. Wet tensile properties of the single filaments were measured via the wet chamber unit of the Favimat+ testing (Textechno, Mönchengladbach, Germany) device. In total, 20 measurements per sample were used for the average calculation.

2.13. Birefringence Measurements

Birefringence measurements were performed at a wavelength of $\lambda = 546$ nm on an Axioscope 5 polarization microscope (Zeiss, Oberkochen, Germany) using a tilt compensator B (Leitz, Oberkochen, Germany). It was used for the determination of the crystalline orientation of the fiber.

2.14. Wide-Angle X-ray Scattering

A diffractometer D/Max Rapid II (Rigaku, The Woodlands, TX, USA) was used for structural analyses. The X-ray tube was operated at 40 kV and 30 mA (Cu K α radiation $\lambda = 1.54059 \text{ \AA}$). A scanning rate of $0.2^\circ/\text{min}$ with a 0.1° scanning step was chosen. The diffractometer was equipped with an image plate detector and a shine monochromator. Fibers were aligned in the sample holder and measured in transmission mode. The degree of crystallinity was calculated according to the peak deconvolution method using pseudo-Voigt functions [31]. Integrated intensities of the crystalline (I_c) and the amorphous reflections (I_a) were determined.

$$I_c = \frac{\sum I_c}{\sum (I_c + I_a)}, \quad (2)$$

The crystallite size (t) was calculated using Scherrer's equation [32].

$$t = \frac{K \cdot \lambda}{B \cdot \cos \theta_b} \quad (3)$$

where the width at half-height of the reflection is B , and the Scherrer factor is K , which depends on the crystallite shape and the Bragg angle (θ_b).

2.15. Water Retention Capacity

Water retention capacity (WRC) was determined according to DIN 53814 [33]. A detailed description is provided elsewhere [34].

2.16. Fibrillation Tests

Wet fibrillation tests were evaluated by fixing single filaments (2.5 cm length) to a frame and placing them in a cylinder containing 20 mL of distilled H₂O and 9 g of zirconia spheres (0.75–1 mm). Testing was performed in a Labomat at 30 °C for 3 h and a rate of 50 rpm. Depending on the counted number of fibrils, fibrillation was classified between 1 and 6 (Table 1). The number of tested fibers was 16 per sample.

Table 1. Classification of the tendency to fibrillate.

| Counted Fibrills | Classification |
|------------------|----------------|
| 0–5 | 1 |
| 6–10 | 2 |
| 11–20 | 3 |
| 21–40 | 4 |
| 41–80 | 5 |
| >80 | 6 |

2.17. Fabric Manufacturing

The resulting fibers were knitted on a multigauged flatbed knitting machine at the Competence Center Staple Fibers, Weaving, and Simulation, DITF Denkendorf.

3. Results and Discussion

3.1. Feedstock

3.1.1. Hemp Feedstock Preparation

The used hemp was grown in rotation with seven other crops (wheat, sunflower, barley, rapeseed, pea, etc.) without using irrigation and chemical fertilizers. As no specific retting is needed for the Irony[®] process, a part of the stalks was picked 2 to 4 days after seed harvest. Dryness was checked to ensure a water content below 15% for storage. A blend of non-retted and medium-retted stalks was processed in a decorticating and defibering

machine (processing speed was set at 1 ton/h). Dust (13%), pure hurd (20%), fiber (23%), tow (5%), and a bulky crushed material (39%) was made of the remaining elements. Bulk material output was analyzed and later turned into pulp (Figure 1) through the application of a new method developed on hemp (patent FR2000801). A cellulose content of $49.5 \pm 0.1\%$ was determined. The hemicellulose and lignin contents were in the range of 16 to 22%. Hurd content was over 70%; the remaining material was mainly bast fibers (primary and tow), and less than 1% of it was ash. The shredded hemp was washed with water in a reactor for 1 h to dissolve pectins, minerals, and other elements. Additionally, the feedstock was softened and prepared for further delignification. After pulping, the lignin content was reduced (Kappa number was 0.8). The final pulp obtained was air-dried. From raw material, the yield was 39%.



Figure 1. (a) Shredded hemp after processing in the decortication line; (b) hemp pulp (HP) as received.

3.1.2. Feedstock Characterization

In general, a DP between 400 and 800 has been reported to be mostly appropriate for spinning [35]. Apart from the DP, the alpha cellulose (R-18) is commonly used to describe the quality of pulp used for cellulosic fiber spinning [22]. Dissolving pulps are characterized by high-purity cellulose (90–99%) with low content of hemicellulose (<4%) and traces of other components. The determined R-18 values of the different pulps were comparable and ranged from 90 to 92%. Small amounts of ash were found (below <0.3 wt. %), typical of high-purity dissolving pulps (Table 2). Inorganic impurities consisted namely of Fe, Na, K, Mg, and Ca. In contrast to the viscose or Lyocell process, where transition metal ions interfere with the processes, e.g., by increasing the radical reaction of NMMO, no negative effects are known for IL-based spinning processes [20,36].

Table 2. Water content, ash content, inorganic impurities, R-18 value, and DP and GPC data of two virgin pulps: wood (WP) and hemp (HP). Values shown in brackets were generated after irradiation.

| Pulp | Water Cont. [%] | Ash Cont. [%] | Fe/Na/K/Mg/Ca [ppm] | R-18 [%] | DP | Mn ^a [kg/mol] | Mw ^b [kg/mol] | D ^c |
|------|-----------------|---------------|---------------------|----------|--------------|--------------------------|--------------------------|----------------|
| WP | 4.1 | 0.11 | 4/220/17/73/3.5 | 92 | 930 (550) | 104 (31) | 613 (324) | 7.0 (10.5) |
| HP | 5.0 | 0.23 | 21/170/9/79/800 | 91 | 660 | 95 | 316 | 3.3 |

^a M_n—Number average molar mass, ^b M_w—Mass average molar mass, ^c D—dispersity.

Besides the purity, the molecular mass distribution is also very important since it has a great influence on the spinnability, as well as on the outcoming fiber properties [37]. To meet the requirements of the HighPerCell[®] process, the degree of polymerization must be

in a certain range for spinning. Therefore, WP was irradiated before dope preparation [21]. Adjusting pulps via electron beam irradiation (EBI) in order to improve the dope and fiber manufacturing was proven to be an accurate and time-saving procedure.

After irradiation, a decreased DP of 550 was measured, while the D (dispersity) value increased to 10.5. HP already showed an applicable DP of 660, and no additional irradiation was necessary to prepare an appropriate spinning dope. These are benefits of the new pulp and the fiber production, respectively. The molecular weight distributions of all pulps used for filament spinning (irradiated WP and the as-received HP) are shown in Figure 2.

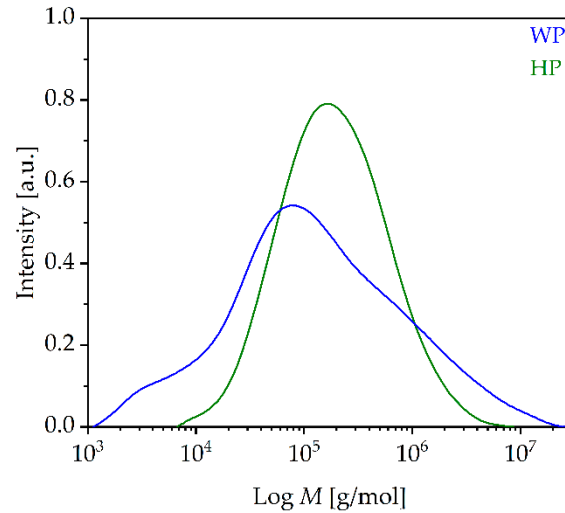


Figure 2. GPC results of pulps (WP (blue), HP (green)) used for spinning dope preparation (WP) and irradiated with 80 kGy).

3.2. Rheology and Fiber Spinning

The determination of the rheology profiles of the cellulose/IL dopes are an approved technique used to determine their spinnability [38,39]. For viscoelastic spinning dopes, a crossover point ($G' = G''$) is expected at a specific frequency (ω_s). Spinning solutions consisting of 12 wt. % cellulose in $[C_2C_1im][Oc]$ displayed non-Newtonian viscous behavior. As a result, a shear-thinning behavior of the viscoelastic fluid was observed, as shown in Figure 3.

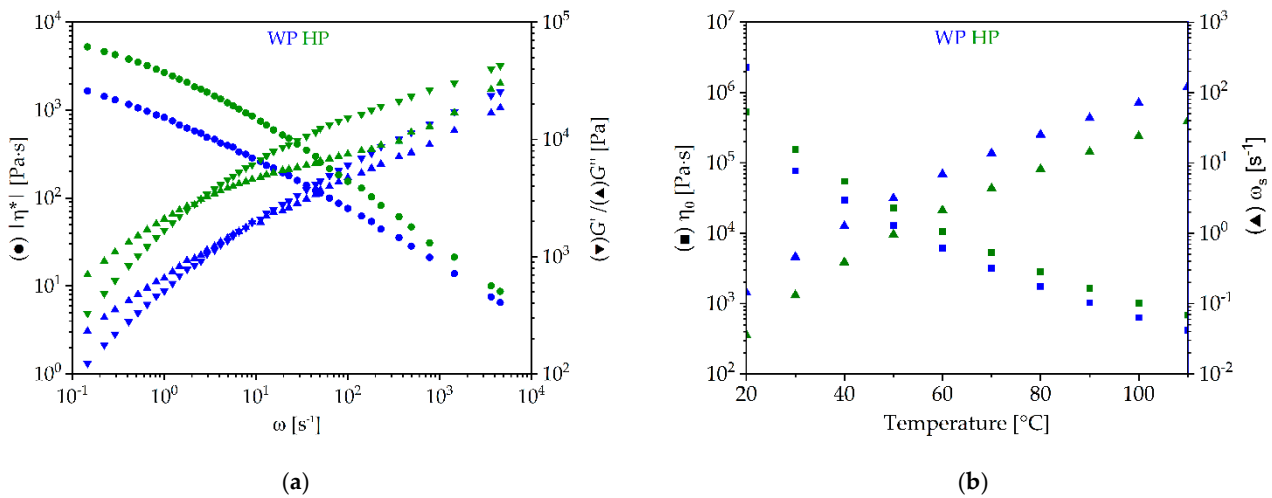


Figure 3. Rheological behavior of the spinning dopes (12 wt. % of WP (blue) and HP (green) in $[C_2C_1im][Oc]$). (a) master curves at reference temperature of 60 °C: In^*I (●), G' (▼), and G'' (▲); (b) rheological parameters η_0 (■) and ω_s (▲) in dependence of temperature.

As expected, the zero shear viscosities (η_0) decreased with increasing temperature, while ω_5 increased. Accordingly, shifts to lower temperatures and lower frequencies were needed to reach the reversible gel point. All solutions possessed an η_0 of around 5000 Pa·s and around 60 °C and cross over points between 2.0 and 6.7 s⁻¹.

3.2.1. Characterization of the Filament

Based on the rheology measurements, spinning was performed at 65 °C, and different draw ratios (DRs) were applied. For all spinning trials, no clogging of the nuzzle was observed, and filaments were spun without any failures. The filaments had an average linear density between 2.2 and 4.2 dtex, which is typical for textile fibers. In comparison to the WP-fibers, HP-fibers showed a higher tenacity (>40 cN/tex vs. 35 cN/tex) and Young's modulus (approx. 2500 vs. approx. 2200 cN/tex) values. Independent of the pulp, all fibers had low elongation between 4 and 6% (Table 3). The prepared filaments (Figure 4) showed similar and acceptable textile properties compared to hemp-based Lyocell fibers [18]. Moreover, the high tenacities of the fibers provide a promising outlook for their application as a replacement material for rayon-based tire cord fibers. Although Michud et al. found that a broad molecular weight distribution of pulp is favourable for fiber spinning, our results do not support this conclusion [27].

Table 3. Mechanical properties (conditioned conditions) of the dry-jet spun HighPerCell[®] filaments spun at 65 °C with different DRs.

| Sample-ID | WP-F | | HP-F | |
|--------------------------|------------|-----------|------------|-----------|
| | 1 | 2 | 1 | 2 |
| DR | 7.7 | 9.6 | 7.7 | 9.6 |
| Fineness [dtex] | 3.1 ± 0.1 | 2.5 ± 0.2 | 4.2 ± 0.3 | 3.2 ± 0.6 |
| Elongation at break [%] | 5.8 ± 1.1 | 4.4 ± 0.5 | 4.4 ± 0.9 | 3.9 ± 0.6 |
| Tenacity [cN/tex] | 35 ± 3 | 35 ± 2 | 41 ± 4 | 41 ± 3 |
| Young's modulus [cN/tex] | 2160 ± 110 | 2230 ± 80 | 2540 ± 110 | 2540 ± 90 |



Figure 4. HP spun filament fibers.

Increasing the spinning temperature to 75 °C had no effect on the mechanical properties of the resulting filaments. Nonetheless, the hemp pulp-based fibers surpassed the mechanical properties of the WP fibers, as shown in Supplementary Materials Table S1. With regard to energy consumption, spinning at a lower temperature without reducing the mechanical fiber properties is a benefit of the IL-spinning process used. In general, such filament properties are paired with high orientation and crystallinity, so both were observed for all materials, as highlighted in Section 3.2.2. This finding was assumed to be the reason why low water retention capacities (WRCs) between 70 and 80% were measured (Figure 5) [34]. The values of the conditioned mechanical properties of the filaments are very close to those of the previously published HighPerCell[®]-based filaments [21,34,40].

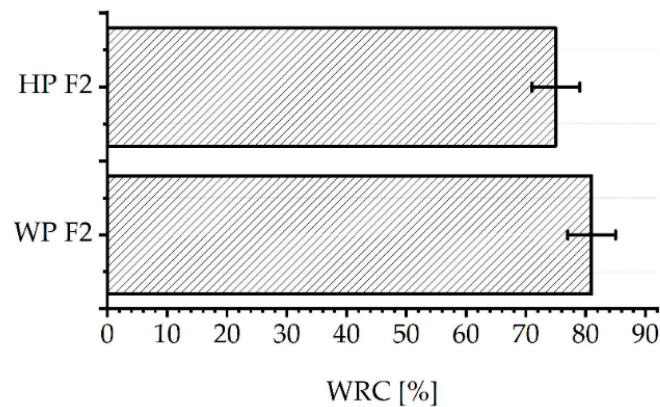


Figure 5. Water retention capacities of different filament types HP-F2 and WP-F2.

Although the filament properties are acceptable, elongation at the break of the fibers should generally be increased to improve the textile properties; higher elongations are required for stretch products, e.g., sportswear. The air-gap spun fibers are pre-orientated, and the elongation at break is highly dependent on the fiber orientation and, therefore, the structure forming process [41]. In fact, fiber orientation has a significant effect on elongation: increased f_t decreases the elongation at break. To improve the elongation at break, HP dope was spun at 75 and 85 °C, and the injection speed was reduced to 1.38 m/min. Figure 6 depicts the average stress–strain curves of HP-based fibers spun at 65 (HP-F1), 75 (HP-75), and 85 °C (HP-85) using the same DR 7.7. The filaments produced under these conditions showed higher elongation, i.e., approximately 7.2% and 9.8% for 75 and 85 °C, respectively.

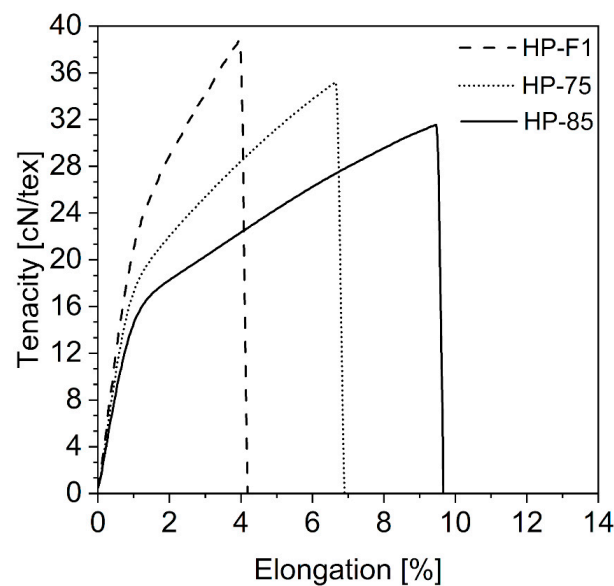


Figure 6. Stress–strain curves of HP-fibers spun at 65 °C (HP-F1), 75 °C (HP-75), and 85 °C (HP-85).

The orientation of the fibers was determined by measuring the birefringence and calculating the total orientation (f_t), as shown in Table 4. The high f_t values are due to the pre-orientation of the cellulose chains during the air-gap spinning [42]. WRCs values of these filaments were comparable to those of samples spun at 65 °C. In addition, mechanical properties under wet conditions were measured. Fibers showed wet state properties typically observed in man-made cellulosic fibers. A decrease in Young's modulus by a factor of 10 was observed. The wet tenacity was reduced by 50%, while an increase in elongation up to 40% was observed, as shown in Table 3.

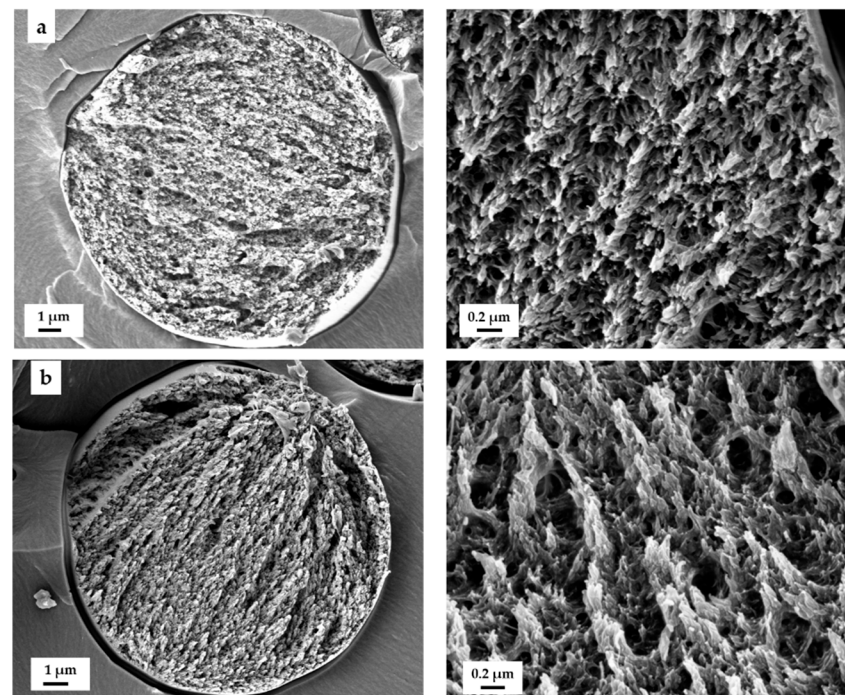
Table 4. Mechanical properties and structure parameters (I_c and f_t) of the dry-jet spun HP filaments at 75 °C and 85 °C.

| Sample-ID | HP-F | |
|---|-----------------|-----------------|
| | −75 | −85 |
| DR | 7.7 | 7.7 |
| Fineness [dtex] | 3.0 ± 0.2 | 3.1 ± 0.2 |
| Cond. ^a elongation at break [%] | 7.1 ± 1.1 | 9.8 ± 1.1 |
| Cond. ^a tenacity [cN/tex] | 37 ± 2 | 33 ± 2 |
| Cond. ^a Young's modulus [cN/tex] | 2130 ± 70 | 1760 ± 100 |
| Wet ^b elongation at break [%] | 11 ± 2 | 12 ± 3 |
| Wet ^b tenacity [cN/tex] | 20 ± 3 | 17 ± 2 |
| Wet ^b Young's modulus [cN/tex] | 230 ± 20 | 170 ± 11 |
| I_c [%] | 65 | 68 |
| Δn | 0.043 | 0.041 |
| f_t | 0.69 ± 0.05 | 0.66 ± 0.04 |
| WRV [%] | 75 | 84 |

^a Conditioned-testing, ^b Wet-testing.

3.2.2. Structure and Morphology

Representative SEM images of a prepared filaments are shown in Figure 7. All filaments had smooth and defect-free surfaces. A circular cross-section showed fibrillar structures and no signs of a skin–core structure. These characteristics have been described for several dry-jet wet spun cellulosic fibers [21,37].

**Figure 7.** SEM micrographs of the fiber fraction of (a) WP-F2 and (b) HP-F2 fibers.

The fiber orientation was quantified via birefringence. All birefringence values (Δn) were measured, and the total orientation (f_t) was calculated (Table S1). All fibers showed a relatively high orientation between 0.65 and 0.67. The crystalline structure of the filaments was analyzed using WAXS measurements. The corresponding diffraction patterns and a typical scattering image are both shown in Figure 8. The cellulosic fibers were crystallized in typical cellulose II structure. Most significant diffraction peaks were observed at

$2\theta \approx 12^\circ$ (-110), 20° (110), 21° (020), and 28° (-113). The crystallinity of the fibers, regardless of the pulp and spinning conditions, was in the range of 65–68%. Curiously, despite the variation in the mechanical properties of the fibers, no significant variations in the total orientation (0.65–0.69) and crystallinity (65–68%) were observed, as shown in Tables S1 and 3. This is probably related to the semicrystalline structure of the cellulose filaments and the resulting measurement accuracy using wide angle X-ray diffraction.

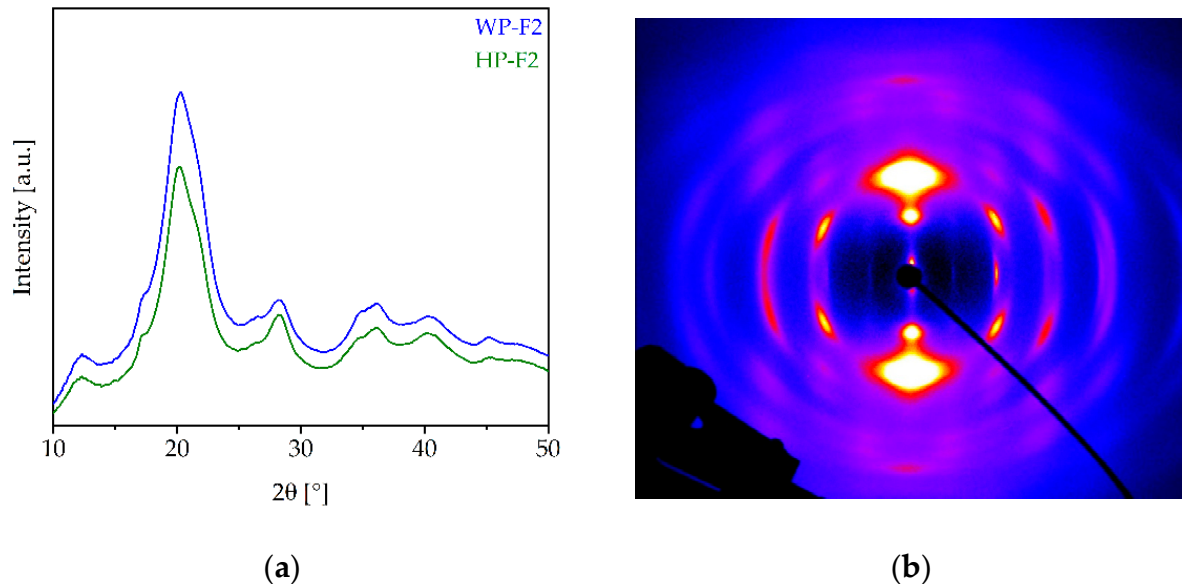


Figure 8. (a) WAXS diffraction patterns of fiber samples: WP-F2 (blue) and HP-F2 (green); (b) scattering image of WP-F2.

Wet fibrillation tests showed that filaments with lower elongation at break values (HP, WP) tended to have high fibrillation values (4–5), while filaments with higher elongation exhibited lower values of 2, as shown in Figure 9. Surprisingly, no correlation between fibrillation behavior and orientation/crystallinity was observed.

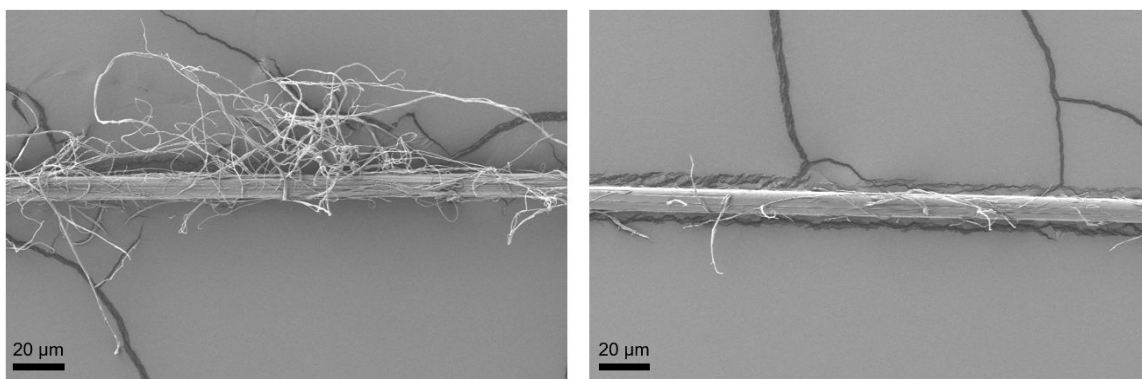


Figure 9. SEM images of fibers after wet fibrillation test: (left) HP-F1 (spun at 65 °C) and (right) HP-F75 (spun at 75 °C).

3.3. Fabric Manufacturing

The HF-75 and HF-85 filaments were used for weaving trials. Both fabrics showed a high structural evenness and possessed a soft touch with low hairiness and a shiny appearance, as shown in Figure 10. SEM imaging revealed that no fiber damage occurred during the weaving process.

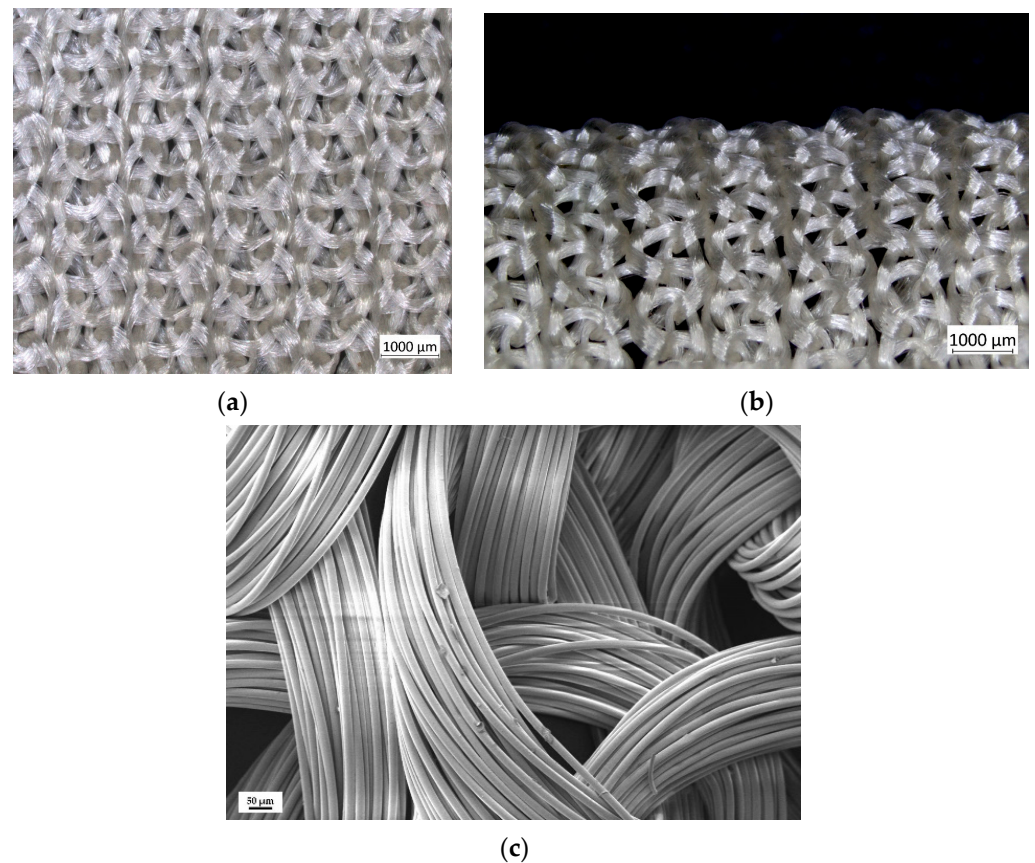


Figure 10. (a,b) images and (c) SEM-image of a woven fabric made of HP-85.

4. Conclusions and Outlook

This study focused on analyzing the potential of hemp pulp produced via a process patented by RBX Créations and its conversion into filaments using HighPerCell[®] technology. Wood dissolving pulp was used as a reference material. Both pulps were suitable for IL-based dope preparation, although the wood required an additional adjustment step of the molecular weight using electron beam irradiation. The developed hemp pulp was of high quality, and no further adjustment was necessary. Filament dry-jet wet spinning was successfully performed with both dopes. Hemp-based filaments surpassed the mechanical properties of wood pulp fibers. Additionally, hemp pulp was used for spinning textile-like fibers with increased elongation. Compared to the high tenacity fibers, the textile fibers tended to fibrillate less frequently. These fibers were also used in the knitting process, resulting in an even fabric with no visible fiber breakage. With regard to textile production, both observations are beneficial.

Furthermore, it should be emphasized that a local available hemp feedstock was combined with two sustainable, energy- and resource-efficient technologies. This is essential for the transition to a circular and sustainable textile value chain. Future work will focus on the up-scaling of pulp production and further optimization of the filament properties in term of elongation. In addition, fiber-to-fiber recycling will be tackled.

Supplementary Materials: The following supporting information can be downloaded via this link: <https://www.mdpi.com/article/10.3390/fib11110090/s1>, Table S1: Degree of crystallinity (I_C) and degree of crystalline orientation (f_t) of the filaments at 65 °C with different DRs and different pulps: wood pulp (WP) and hemp pulp (HP) via RBX.

Author Contributions: Conceptualization: A.O. and M.P.V.; methodology, R.B.; formal analysis, M.P.V. and R.B.; investigation: A.O., R.B., A.R. and C.R.; writing—original draft preparation: M.P.V. and A.R.; writing—review and editing: A.O., C.R. and F.H.; visualization: A.O. and M.P.V.; supervi-

sion: A.O.; project administration: A.R. and A.O.; funding acquisition: A.O. and A.R. All authors have read and agreed to the published version of the manuscript.

Funding: This research project (name: IHMDILT) was funded by the ELIIT Partnership Project in the framework of the COSME Programme of the European Union for the Competitiveness of Enterprises and Small- and Medium-Sized Enterprises (SMEs).

Data Availability Statement: Complete results from experimental testing are provided.

Acknowledgments: The authors would like to thank Sabine Henzler and Ulrich Hageroth for performing SEM and taking birefringence measurements. In addition, the authors thank Patricija Tomasic for wet fibrillation testing and Uwe Röder for performance of the knitting trails.

Conflicts of Interest: The authors declare no conflict of interest.

References

- Horne, M.R.L. *Handbook of Natural Fibres*; Kozłowski, R.M., Ed.; Woodhead Publishing: Cambridge, UK, 2012; Volume 1, pp. 114–145.
- Manian, A.P.; Cordin, M.; Pham, T. Extraction of cellulose fibers from flax and hemp: A review. *Cellulose* **2021**, *28*, 8275–8294. [CrossRef]
- Cultivation. Available online: https://www.interchanvre.org/la_culture#les_chiffres_cles (accessed on 30 August 2023).
- Haemmerle, F.M. The Cellulose Gap (The Future of Cellulose Fibers). *Lenzing. Ber.* **2011**, *89*, 12–21.
- El Seoud, O.A.; Kostag, M.; Jedvert, K.; Malek, N.I. Cellulose Regeneration and Chemical Recycling: Closing the “Cellulose Gap” Using Environmentally Benign Solvents. *Macromol. Mater. Eng.* **2020**, *305*, 1900832. [CrossRef]
- Bredereck, K.; Hermanutz, F. Man-made cellulose. *Rev. Prog. Color. Relat. Top.* **2005**, *35*, 59–75. [CrossRef]
- Sayyed, A.J.; Deshmukh, N.A.; Pinjari, D.V. A critical review of manufacturing processes used in regenerated cellulosic fibres: Viscose, cellulose acetate, cuprammonium, LiCl/DMAc, ionic liquids, and NMMO based lyocell. *Cellulose* **2019**, *26*, 2913–2940. [CrossRef]
- Taokaew, S.; Kriangkrai, W. Recent Progress in Processing Cellulose Using Ionic Liquids as Solvents. *Polysaccharides* **2022**, *3*, 671–691. [CrossRef]
- Felgueiras, C.; Azoia, N.G.; Goncalves, C.; Gama, M.; Dourado, F. Trends on the Cellulose-Based Textiles: Raw Materials and Technologies. *Front. Bioeng. Biotechnol.* **2021**, *9*, 608826. [CrossRef]
- Paulitz, J.; Sigmund, I.; Kosan, B.; Meister, F. Lyocell fibers for textile processing derived from organically grown hemp. *Procedia Eng.* **2017**, *200*, 260–268. [CrossRef]
- Makarov, I.S.; Golova, L.K.; Smyslov, A.G.; Vinogradov, M.I.; Palchikova, E.E.; Legkov, S.A. Flax Noils as a Source of Cellulose for the Production of Lyocell Fibers. *Fibers* **2022**, *10*, 45. [CrossRef]
- Lawson, L.; Degenstein, L.M.; Bates, B.; Chute, W.; King, D.; Dolez, P.I. Cellulose Textiles from Hemp Biomass: Opportunities and Challenges. *Sustainability* **2022**, *14*, 15337. [CrossRef]
- Seile, A.; Spurina, E.; Sinka, M. Reducing Global Warming Potential Impact of Bio-Based Composites Based of LCA. *Fibers* **2022**, *10*, 79. [CrossRef]
- McDonald, H.; Frelth-Larsen, A.; Lóránt, A.; Duin, L.; Andersen, S.P.; Costa, G.; Bradley, H. *Carbon farming, Making Agriculture Fit for 2030*; Policy Department for Economic, Scientific and Quality of Life Policies Directorate-General for Internal Policies; European Union: Luxemburg, 2021; pp. 1–67.
- Conchedda, G.; Tubiello, F.N. *Emissions Due to Agriculture. Global, Regional and Country Trends 2000–2018*; Environmental team, F. S. D., FAOSTAT Analytical Brief Series, Eds.; FAO: Rome, Italy, 2020; Volume 18, pp. 1–67.
- da Silva, M.G.; Lisbôa, A.C.L.; Hoffmann, R.; da Cunha Kemerich, P.D.; de Borba, W.F.; Fernandes, G.D.Á.; de Souza, É.E.B. Greenhouse gas emissions of rice straw-to-methanol chain in Southern Brazil. *J. Environ. Chem. Eng.* **2021**, *9*, 105202–105215. [CrossRef]
- Jiang, X.; Bai, Y.; Chen, X.; Liu, W. A review on raw materials, commercial production and properties of lyocell fiber. *J. Bioresour. Bioprod.* **2020**, *5*, 16–25. [CrossRef]
- Thümmel, K.; Fischer, J.; Fischer, S.; Kosan, B.; Meister, F. Lyohemp™ Fibres from Hemp Shive Dissolving Pulp. *Lenzing. Ber.* **2022**, *97*, 25–31.
- Rissanen, M.; Schlapp-Hackl, I.; Sawada, D.; Raisio, S.; Ojha, K.; Smith, E.; Sixta, H. Chemical recycling of hemp waste textiles via the ionic liquid based dry-jet-wet spinning technology. *Text. Res. J.* **2022**, *93*, 2545–2557. [CrossRef]
- Hermanutz, F.; Vocht, M.P.; Buchmeiser, M.R. *Commercial Applications of Ionic Liquids. Green Chemistry and Sustainable Technology*; Shiflett, M., Ed.; Springer: Cham, Switzerland, 2020; Volume 1, pp. 227–259.
- Vocht, M.P.; Beyer, R.; Thomasic, P.; Müller, A.; Ota, A.; Hermanutz, F.; Buchmeiser, M.R. High-performance cellulosic filament fibers prepared via dry-jet wet spinning from ionic liquids. *Cellulose* **2021**, *28*, 3055–3067. [CrossRef]
- Fechter, C.; Fischer, S.; Reimann, F.; Breid, H.; Heinze, T. Influence of pulp characteristics on the properties of alkali cellulose. *Cellulose* **2020**, *27*, 7227–7241. [CrossRef]

23. DIN 54355:1977-11; Testing of Pulp; Determination of the Stability of Pulp against Sodium Hydroxide Solution (Alkali Resistance). Deutsches Institut Fur Normung E.V.: Berlin, Germany, 1977.
24. DIN 54370:2007-06; Testing of Paper and Board—Determination of the Residue on Ignition. Deutsches Institut Fur Normung E.V.: Berlin, Germany, 2007.
25. DIN EN ISO 11885:2009-09; Water Quality—Determination of Selected Elements by Inductively Coupled Plasma Optical Emission Spectrometry (ICP-OES) (ISO 11885:2007), German version EN ISO 11885:2009. ISO: Geneva, Switzerland, 2009.
26. Meister, F.; Kosan, B. A tool box for characterization of pulps and cellulose dopes in Lyocell technology. *Nord. Pulp Paper Res. J.* **2015**, *30*, 112–120. [[CrossRef](#)]
27. Michud, A.; Hummel, M.; Sixta, H. Influence of molar mass distribution on the final properties of fibers regenerated from cellulose dissolved in ionic liquid by dry-jet wet spinning. *Polymer* **2015**, *75*, 1–9. [[CrossRef](#)]
28. DIN 54270-1:1976-09; Testing of Textiles; Determination of the Limit-Viscosity of Celluloses, Principles. Deutsches Institut Fur Normung E.V.: Berlin, Germany, 1976.
29. Gahleitner, M.; Sobczak, R. Importance of the zero shear viscosity determination to the modelling of flow curves. *Kunst.-Ger. Plast.* **1989**, *79*, 1213–1216.
30. DIN EN ISO 5079:2021-02; Textile Fibres—Determination of Breaking Force and Elongation at Break of Individual Fibres (ISO 5079:2020). German version EN ISO 5079:2020. ISO: Geneva, Switzerland, 2021.
31. Rongpipi, S.; Ye, D.; Gomez, E.D.; Gomez, E.W. Progress and Opportunities in the Characterization of Cellulose—An Important Regulator of Cell Wall Growth and Mechanics. *Front Plant Sci.* **2018**, *9*, 1894. [[CrossRef](#)] [[PubMed](#)]
32. Scherrer, P. Bestimmung der Größe und der inneren Struktur von Kolloidteilchen mittels Röntgenstrahlen. *Nachrichten von der Gesellschaft der Wissenschaften zu Göttingen Mathematisch-Physikalische Klasse* **1918**, *1918*, 98–100.
33. DIN 53814:1974-10; Testing of Textiles; Determination of Water Retention Power of Fibres and Yarn Cuttings. Deutsches Institut Fur Normung E.V.: Berlin, Germany, 1974.
34. Ota, A.; Beyer, R.; Hageroth, U.; Müller, A.; Tomasic, P.; Hermanutz, F.; Buchmeiser, M.R. Chitin/cellulose blend fibers prepared by wet and dry-wet spinning. *Polym. Adv. Technol.* **2020**, *32*, 335–342. [[CrossRef](#)]
35. Abels, F.; Cwik, T.; Beyer, R.; Hermanutz, F. Process for the Preparation of Polymer Fibers from Polymers Dissolved in Ionic Liquids by Means of an Air Gap Spinning Process. Patent WO2017/137284AI, 17 August 2017.
36. Zhang, S.; Chen, C.; Duan, C.; Hu, H.; Li, H.; Li, J.; Liu, Y.; Ma, X.; Stavik, J.; Ni, Y. Regenerated cellulose by the lyocell process, a brief review of the process and properties. *Bioresources* **2018**, *13*, 1–16. [[CrossRef](#)]
37. Moriam, K.; Sawada, D.; Nieminen, K.; Hummel, M.; Ma, Y.; Rissanen, M.; Sixta, H. Towards regenerated cellulose fibers with high toughness. *Cellulose* **2021**, *28*, 9547–9566. [[CrossRef](#)]
38. Ingildeev, D.; Effenberger, F.; Bredereck, K.; Hermanutz, F. Comparison of direct solvents for regenerated cellulosic fibers via the lyocell process and by means of ionic liquids. *J. Appl. Polym. Sci.* **2013**, *128*, 4141–4150. [[CrossRef](#)]
39. Olsson, C.; Westman, G. Wet spinning of cellulose from ionic liquid solutions—viscometry and mechanical performance. *J. Appl. Polym. Sci.* **2013**, *127*, 4542–4548. [[CrossRef](#)]
40. Vocht, M.P.; Ota, A.; Frank, E.; Hermanutz, F.; Buchmeiser, M.R. Preparation of Cellulose-Derived Carbon Fibers Using a New Reduced-Pressure Stabilization Method. *Ind. Eng. Chem. Res.* **2022**, *61*, 5191–5201. [[CrossRef](#)]
41. Lenz, J.; Schurz, J.; Wrentschur, E. On the Elongation Mechanism of Regenerated Cellulose Fibres. *Holzforschung* **1994**, *48*, 72–76. [[CrossRef](#)]
42. Mortimer, S.A.; Peguy, A.A. The influence of air-gap conditions on the structure formation of lyocell fibers. *J. Appl. Polym. Sci.* **1998**, *60*, 1747–1756. [[CrossRef](#)]

Disclaimer/Publisher’s Note: The statements, opinions and data contained in all publications are solely those of the individual author(s) and contributor(s) and not of MDPI and/or the editor(s). MDPI and/or the editor(s) disclaim responsibility for any injury to people or property resulting from any ideas, methods, instructions or products referred to in the content.